

Predicting Skin Permeability from Complex Chemical Mixtures: Dependency of Quantitative Structure Permeation Relationships on Biology of Skin Model Used

Jim E. Riviere¹ and James D. Brooks

Center for Chemical Toxicology Research and Pharmacokinetics, North Carolina State University, Raleigh, North Carolina 27606

¹To whom correspondence should be addressed at Center for Chemical Toxicology Research and Pharmacokinetics, North Carolina State University, 4700 Hillsborough Street, Raleigh, NC 27606. Fax: (919) 513-6358. E-mail: jim_riviere@ncsu.edu.

Received June 14, 2010; accepted October 7, 2010

Dermal absorption of topically applied chemicals usually occurs from complex chemical mixtures; yet, most attempts to quantitate dermal permeability use data collected from single chemical exposure in aqueous solutions. The focus of this research was to develop quantitative structure permeation relationships (QSPR) for predicting chemical absorption from mixtures through skin using two levels of *in vitro* porcine skin biological systems. A total of 16 diverse chemicals were applied in 384 treatment mixture combinations in flow-through diffusion cells and 20 chemicals in 119 treatment combinations in isolated perfused porcine skin. Penetrating chemical flux into perfusate from diffusion cells was analyzed to estimate a normalized dermal absorptive flux, operationally an apparent permeability coefficient, and total perfusate area under the curve from perfused skin studies. These data were then fit to a modified dermal QSPR model of Abraham and Martin including a sixth term to account for mixture interactions based on physical chemical properties of the mixture components. Goodness of fit was assessed using correlation coefficients (r^2), internal and external validation metrics (q_{LOO}^2 , $q_{\text{L25\%}}^2$, q_{EXT}^2), and applicable chemical domain determinations. The best QSPR equations selected for each experimental biological system had r^2 values of 0.69–0.73, improving fits over the base equation without the mixture effects. Different mixture factors were needed for each model system. Significantly, the model of Abraham and Martin could also be reduced to four terms in each system; however, different terms could be deleted for each of the two biological systems. These findings suggest that a QSPR model for estimating percutaneous absorption as a function of chemical mixture composition is possible and that the nature of the QSPR model selected is dependent upon the biological level of the *in vitro* test system used, both findings having significant implications when dermal absorption data are used for *in vivo* risk assessments.

Key Words: chemical mixtures; percutaneous/dermal absorption; quantitative structure-activity relationships (QSAR); QSPR; skin permeability; *in vitro* models; pesticide risk assessment.

Predicting the degree of dermal absorption of topically exposed chemicals is an important issue in both environmental and occupational risk assessment. Most risk assessment approaches are based on data obtained from dosing chemicals neat or in simple aqueous vehicles, yet most exposures are to more complex mixtures. Numerous studies have demonstrated that vehicles may have significant effects on modulating chemical absorption (Bliss, 1939; Cross *et al.*, 2001; Idson, 1983; Qiao *et al.*, 1996; Rosado *et al.*, 2003; Sloan *et al.*, 1986). In fact, this is the prime strategy behind developing pharmaceutical formulations (Augustijns and Brewster, 2007). Today, there is little doubt that vehicle and formulation components modulate dermal absorption or transdermal delivery of topically applied drugs and solutes. Despite the intellectual certainty of this effect, most attempts in risk assessment modeling to quantitate dermal absorption using quantitative structure permeability relationships (QSPR) are based on defining linear free-energy relationships (LFER) using data obtained from single compound exposure in simple aqueous solutions (Abraham and Martins, 2004; EPA, 2004; Geinoz *et al.*, 2004; Hostynek and Magee, 1997; Neuman, 2008; Potts and Guy, 1992).

Because the vast majority of occupational and environmental exposure to chemicals is in the form of mixtures, understanding the mechanism operative in modulating chemical penetration into and absorption through the skin is crucial to predicting toxicological effects. Limited work has been done to broadly incorporate the effect of mixture interactions seen in more complex but realistic formulations (Baynes *et al.*, 2008; Gregoire *et al.*, 2009). What is required for realistic risk assessments on topical mixtures is a general approach that at a minimum indicates whether a specific mixture would be expected to increase or decrease absorption through the skin. A quantitative indication of the extent of modulation would be optimal.

We have previously reported on a straightforward approach to incorporate physiochemical properties of a mixture into existing QSPR models. These studies were focused on an

TABLE 1
Identity, Specific Activity, Purity, and Source of Study Compounds

| Compound | mCi/mmol | Purity (%) | Source |
|---|------------------|------------|--------|
| Atrazine-ring-UL-14C | 15.1 | 98.1 | SCC |
| MethylParathion-ring-UL-14C | 13.8 | 99.5 | SCC |
| 4-Nitrophenol-UL-14C | 6.4 | 99.6 | SCC |
| Parathion-ring-UL-14C | 9.2 | 97.1 | SCC |
| Pentachlorophenol-ring-UL-14C | 11.9 | 98 | SCC |
| Permethrin-benzyl-ring-UL-14C | 10.9 | 96.1 | SCC |
| Phenol-UL-14C | 9 | 98.5 | SCC |
| Simazine-ring-UL-14C | 15.5 | 99 | SCC |
| Chlorpyrifos [pyridine-2,6-14C] | 32 | 99 | ARC |
| Fenthion-ring-UL-14C | 55 | 98.5 | ARC |
| Propazine-ring-UL-14C | 15 | 96.6 | ARC |
| 1,3,5-Triethyl hexahydro-S-triazine [methylene-14C] | 10 | 98.6 | ARC |
| Ricinoleic acid [12-3H] | 20,000 | 99 | ARC |
| Caffeine [8-14C] | 52 | 99 | ARC |
| Octanol [1-14C] | 5 | 99 | ARC |
| Testosterone [4-14C] | 55 | 99 | ARC |
| Codeine [N-methyl-14C] | 50 | 99 | ARC |
| 4-Chlorophenol [14C(U)] | 20 | 99 | ARC |
| 4-Cyanophenol [cyano-14C] | 20 | 99 | ARC |
| 4-Phenoxyphenol [phenol-ring-14C(U)] | 77 | 99 | ARC |
| 2,4-Dimethylphenol [phenol-ring-14C(U)] | 75 | 99 | ARC |
| Chlorfenvinphos [ethyl-1-14C] | 7.9 | 99.7 | IOI |
| Dimethoate [carbonyl-14C] | 6.6 | 98.2 | IOI |
| Metribuzin [ring-6-14C] | 10.6 | 98.7 | IOI |
| Diazinon [pyrimidine-6-14C] | 53 | 96.3 | MB |
| p-Nonylphenol-ring-14C | 76.6 | | BDR |
| Sodium 2-dodecylbenzene sulfonate-ring-UL-14C | 50.77 | 99.1 | WL |
| DEET | Not radiolabeled | 98 | CSC |
| Absolute ethyl alcohol (200 proof) | Not radiolabeled | 100 | AA |
| Propylene glycol | Not radiolabeled | 99 | SCC |
| Sodium lauryl sulfate | Not radiolabeled | 99 | SCC |
| Methylnicotinic acid | Not radiolabeled | 99 | SCC |
| Water | Not radiolabeled | | House |

Note. SCC, obtained from Sigma Chemical Co., St Louis, MO; ARC, obtained from American Radiolabeled Chemicals, Inc., St Louis, MO; IOI, obtained from Institute of Isotopes Co., Ltd. Budapest, Hungary; MB, obtained from Moravék Biochemicals, Inc., Brea, CA; BDR, obtained from BioDynamics Radiochemicals, Billingham, UK; WL, obtained from Wizard Laboratories, Sacramento, CA; CSC, obtained from Chem Service Company, West Chester, PA; AA, obtained from Aaper Alcohol and Chemical Co. Shelbyville, KY. Water was distilled in our in-house still. N,N diethyl-*m*-toluamide (DEET) was not radiolabeled and was analyzed via high performance liquid chromatography (HPLC).

initial set of 12 penetrants in 24 mixtures for 288 treatment combinations (complete factorial experimental design) based on data collected using *in vitro* porcine skin flow-through (PSFT) diffusion cells and the five descriptor linear free-energy QSPR relationship of Abraham and Martins (2004) (Riviere and Brooks, 2005). This approach was subsequently expanded using data from the more biologically sophisticated isolated perfused porcine skin flap (IPPSF) model (10 penetrants in five

mixtures for 50 treatment combinations). The IPPSF is an *ex vivo* biologically intact perfused tissue preparation that has previously been shown to correlate to *in vivo* human dermal absorption (Riviere, 2006; Riviere *et al.*, 1986, 1992; Riviere and Monteiro-Riviere, 1991; Wester *et al.*, 1998). The use of this model assures that chemical mixture interactions involving the stratum corneum as well as viable epidermis and dermis would be detected because such interactions which would occur *in vivo* could confound solvatochromatic interactions detected using nonbiological systems, necessitating that such an approach be used if the goal is to reliably predict *in vivo* effects. The approach's applicability to other QSPR models was assessed by also applying it to the QSPR models of Hostynek and Magee (1997) as well as Potts and Guy (1992) (Riviere and Brooks, 2007).

The present study significantly expands on this analysis by increasing the number of penetrants studied in the *in vitro* porcine skin diffusion cells to 16 for a total of 384 treatment combinations and in the IPPSF to 20 penetrants dosed in a total of 119 treatment combinations. These larger data sets expand the chemical inference space to which such analyses can be applied but more importantly allow for comparison between QSPR model structures across experimental systems and begin to offer validation of the concept that such an approach is applicable to modifying the dermal risk assessment paradigm now rooted in simple single chemical aqueous exposures. The goal of this analysis was to confirm that this approach is valid across a more diverse group of chemicals and determines if mixture-based QSPR models can be extrapolated across *in vitro* model systems of different biological complexity.

MATERIALS AND METHODS

Study chemicals. The chemical compounds used in the studies are listed in Table 1 along with their specific radioactivity, purity, and source.

In vitro PSFT diffusion cell. The flow-through diffusion cell was used to perfuse porcine skin obtained from the dorsal area of weanling female Yorkshire pigs (*Sus scrofa*) according to protocols approved by the North Carolina State University Institutional Animal Care and Use Committee (Bronaugh and Stewart, 1985; Chang and Riviere, 1991). Skin was dermatomed to a thickness of 500 μm with a Padgett Dermatome (Padgett Instruments, Inc., Kansas City, MO). Each circular skin disk was punched to provide a dosing surface area of 0.64 cm^2 and then placed into a two-compartment Teflon flow-through diffusion cell (Crowne Glass, Somerville, NJ). Skin was perfused using a Krebs-Ringer bicarbonate buffer spiked with dextrose and bovine serum albumin. The skin was topically dosed nonoccluded with 20 μl of one of 16 marker penetrant compounds listed in Table 2 formulated in one of 24 specified mixtures also listed in Table 2. This resulted in a training set of 384 treatments with $n = 4\text{--}5$ replicates per treatment designed as a randomized complete factorial experiment. The target dose concentration was 20 $\mu\text{g}/\text{cm}^2$. Perfusate flow rate was 4 ml/h, and perfusate samples were collected every 15 min for 2 h and every hour thereafter until the end of the 8-h dosing period.

Because we used finite doses, pseudo-steady state flux was determined from the slope of the cumulative perfusate flux profile versus time. The concentration was the initial chemical concentration in the vehicle at the start of the

TABLE 2
Identity of 16 Training Set Compounds Investigated in 384
Mixtures in the PSFT

| Substituted phenols | Organophosphates | Triazine herbicides | Selected compounds |
|--|------------------|------------------------|--------------------|
| Phenol | Methylparathion | Atrazine | Caffeine |
| Pentachlorophenol | Ethylparathion | Propazine | Octanol |
| 4-Nitrophenol | Chlorpyrifos | Simazine | Testosterone |
| 4-Nonylphenol | Fenthion | Triazine | Codeine |
| Composition of 24 training set mixtures investigated in the PSFT | | | |
| EtOH | | PG | |
| EtOH + MNA | | PG + MNA | |
| EtOH + SLS | | PG + SLS | |
| EtOH + MNA + SLS | | PG + MNA + SLS | |
| EtOH + water | | PG + water | |
| EtOH + water + MNA | | PG + water + MNA | |
| EtOH + water + SLS | | PG + water + SLS | |
| EtOH + water + MNA + SLS | | PG + water + MNA + SLS | |
| EtOH + PG | | Water | |
| EtOH + PG + MNA | | Water + MNA | |
| EtOH + PG + SLS | | Water + SLS | |
| EtOH + PG + MNA + SLS | | Water + MNA + SLS | |

Note. MNA, methylnicotinic acid; PG, propylene glycol (1,2-propanediol); SLS, sodium lauryl sulfate.

experiment. We assessed percutaneous absorption by calculating flux into perfusate normalized to applied surface concentration. This generates an operational or apparent permeability constant (k_p^*) for a penetrant from a specific vehicle exposure scenario that parallels calculation of a formal k_p defined by Fick's First Law of Diffusion determined using infinite dosing under occluded conditions from a single vehicle. We are using k_p^* as an operational absorption metric that normalizes flux by the applied surface concentration at application time. We conducted these studies using finite doses under nonoccluded conditions to model the occupational exposure scenario, which unfortunately does not allow for preventing loss of volatile compounds.

The validation set is made up of PSFT experiments run prior to and with a similar experimental design to that of the training set. Table 3 lists the identity of seven validation set compounds investigated in 89 mixtures created from differing combinations of 14 validation set mixture components in the PSFT.

IPPSF studies. The IPPSF is a single-pedicle, axial pattern tubed skin flap obtained from the abdomen of female weanling Yorkshire pigs (*S. scrofa*). This

TABLE 3
Identity of Seven Validation Set Compounds Investigated in 89
Mixtures in the PSFT

| Benzidine | LAS | Permethrin |
|--|---------------------|------------------|
| Carbaryl | Pentachlorophenol | Triazine |
| DEET | | |
| Composition of 14 validation set mixture components investigated in the PSFT | | |
| Acetone | Mineral oil | SLS |
| DEET | MNA | Triazine |
| DMSO | Permethrin | Triethanol amine |
| EtOH | Polyethylene glycol | Water |
| LAS | Ricinoleic acid | |

Note. DEET, N,N diethyl-*m*-toluamide; DMSO, Dimethylsulfoxide; LAS, linear alkylbenzene sulfonate; MNA, methylnicotinic acid; SLS, sodium lauryl sulfate.

model system contains a functional microcirculation and an anatomically intact and viable epidermis and dermis. Two flaps per animal, each lateral to the ventral midline, were created in a single surgical procedure using protocols approved by the North Carolina State University Institutional Animal Care and Use Committee. The procedure involved surgical creation of the flap (measuring 4×12 cm) perfused primarily by the caudal superficial epigastric artery and its associated paired venae comitantes followed by arterial cannulation and harvest in 48 h (Bowman *et al.*, 1991). The IPPSF was then transferred to a perfusion apparatus that is a custom-designed temperature- and humidity-regulated chamber. Perfusion media consisted of a modified Krebs-Ringer bicarbonate buffer spiked with dextrose and bovine serum albumin. Normal perfusate flow rate was maintained at 1 ml/min/flap (3–7 ml/min/100 g) with a mean arterial pressure ranging from 30–70 mmHg, targets consistent with *in vivo* values reported in the literature. Viability for up to 24 h has been confirmed through biochemical studies and extensive light and transmission electron microscopy studies (Monteiro-Riviere *et al.*, 1987). Radiolabeled compounds were topically applied in their respective vehicle under ambient, nonoccluded conditions. These techniques are fully described in the literature (Riviere *et al.*, 1986; Riviere and Monteiro-Riviere, 1991).

The skin was topically dosed with 100 μ l of one of 20 marker penetrant compounds listed in Table 4 formulated in one of five or six specified mixtures also listed in Table 4. This resulted in a training set of 119 treatments with $n = 3$ replicates per treatment. The target dose concentration was 20 μ g/cm². Perfusate flow rate was 1 ml/min, and perfusate samples were collected every 15 min for 2 h and every half hour thereafter until the end of the 8-h dosing period.

For the IPPSF experiments, perfusate flux logAUC (area under the curve) rather than $\log k_p^*$ was employed because it better represents the total transdermal flux across this more complex, vascularized model system. AUC (%D h/ml) was calculated using the trapezoidal rule, wherein the mean of the concentration of two adjacent time points was multiplied by the elapsed time of those two samples and added to the remaining means. Table 5 lists the identity of 10 validation set compounds investigated in 40 mixtures created from combinations of the six validation set mixture components in the IPPSF.

Radioisotope counting. Compounds used in these studies were radio-labeled (¹⁴C), and the perfusate flux was determined using liquid scintillation counting on a Packard 1900TR Tricarb Liquid Scintillation Counter (Packard Instruments, Inc., Downers Grove, IL).

QSPR modeling approach. Multiple regression analysis was carried out using SAS 9.1 for Windows (SAS Institute, Cary, NC). We have used stepwise regression (SAS 9.1) with each model in addition to the two or five parameters established by the model authors to determine the best mixture factor (MF) for each biological system. The two parameters utilized in the model of Potts and Guy (1992) are $\log K_{ow}$ (log of the octanol:water partition coefficient) and the molecular weight (MW). The five model parameters utilized in the model of Abraham and Martins (2004) are $\Sigma \alpha_2^H$ (hydrogen bond donor acidity), $\Sigma \beta_2^H$ (hydrogen bond acceptor basicity), π_2^H (dipolarity/polarizability), R_2 (excess molar refractivity), and V_x (McGowan volume). The MF is a third term added to the model of Potts and Guy (1992) or a sixth term added to the model of Abraham and Martins to account for mixture interactions based on physical chemical properties of the mixture components. Goodness of fit was assessed using coefficients of variation (r^2) and internal and external validation metrics (q_{LOO}^2 , $q_{L25\%}^2$, and q_{EXT}^2). Stepwise regression was used to select the best MF, based on r^2 values, from among the following physicochemical properties: water solubility, Henry's law constant, polarizability, partition coefficient, LogD, ovality, MW, molecular volume, topical polar surface area (TPSA), refractive index, molar refractivity, hydrogen bond acceptors, hydrogen bond donors, boiling point, melting point (MP), boiling point minus MP, vapor pressure, Connolly accessible area, Connolly molecular area, Connolly solvent excluded volume, pKa, number of atoms, number of rotatable bonds, Lipinski number, fugacity, bioconcentration factor, and atmospheric hydroxyl radical rate constant.

TABLE 4
Identity of 20 Training Set Compounds Investigated in 119
Mixtures in the IPPSF

| | | | | | |
|---|-----------------------------|----------------------------|-------------|------------|-----------|
| <i>Substituted phenols</i> | <i>Organophosphates</i> | <i>Triazine herbicides</i> | | | |
| Phenol ^a | Methylparathion | Atrazine | | | |
| Pentachlorophenol ^a | Ethylparathion ^a | Propazine ^a | | | |
| 4-Nitrophenol ^a | Chlorpyrifos | Simazine ^a | | | |
| 4-Nonylphenol | Fenthion ^a | Triazine ^a | | | |
| Composition of five training set mixtures investigated in the IPPSF | | | | | |
| EtOH | EtOH + water | Water | Water + SLS | PG | |
| 4-Chlorophenol | | Diazinon | | Metribuzin | |
| 4-Cyanophenol | | Chlorfenvinphos | | | |
| 4-Phenoxyphenol | | Dimethoate | | | |
| 2,4-Dimethylphenol | | | | | |
| Composition of six training set mixtures investigated in the IPPSF | | | | | |
| EtOH | EtOH + water | Water | Water + SLS | EtOH + MNA | MNA + SLS |

Note. Pentachlorophenol was also investigated in EtOH + MNA, EtOH + water + MNA, PG + SLS, and water + PG. 4-Nonylphenol was not investigated in PG. MNA, methylnicotinic acid; SLS, sodium lauryl sulfate.

^aEight compounds were also investigated in water + linear alkylbenzene sulfonate.

In Tables 6, 7, and 8, we report each model without and with the MFs. Tabulated statistics include the number of treatments (n), the coefficient of variation (r^2), the square of the correlation coefficients adjusted to the number of degrees of freedom (adj. r^2), the cross-validation square of the correlation coefficients using the “leave-one-out” (q_{LOO}^2) and the “leave-a-random-25%-out” ($q_{L25\%}^2$) techniques, the standard deviation (s), and the Fischer’s statistical test (F) for each equation. Also listed in Tables 6, 7, and 8 are the p values associated with each model component. The capability of the models to predict the treatments of the validation set was determined by the external validation parameter (q_{EXT}^2). The $q_{EXT}^2 = 1 - \text{PRESS}/\text{SD}$, where PRESS is the sum of the squared differences between the observed data and the predicted data for each treatment in the validation set and SD is the sum of the squared differences between the observed validation set treatments and the mean observed data of the training set treatments.

The Williams’ Plot was used to visualize the applicability domain (AD). It is a plot of the standardized cross-validated residuals versus the leverage hat diagonal values (h). The standardized cross-validated residuals result from the q_{LOO}^2 calculations. The hat diagonal is calculated using the hat matrix: $H = X(X^T X)^{-1} X^T$, where $H = Y^{\wedge}$ (“y-hat” the predicted value of y), X is the ($m \times n$) matrix, and X^T is the transpose of the X matrix ($n \times m$). X is defined as

TABLE 5
Identity of 10 Validation Set Compounds Investigated in 40
Mixtures in the IPPSF

| | | |
|--|-----------------------------|--------------|
| 4-Nitrophenol | Octanol | Permethrin |
| Carbaryl | <i>p</i> -Aminobenzoic acid | Phenol |
| Ethylparathion | Pentachlorophenol | Theophylline |
| Methyl salicylate | | |
| Composition of six validation set mixture components investigated in the IPPSF | | |
| Acetone | EtOH | SLS |
| DEET | MNA | Water |

Note. DEET, N,N diethyl-*m*-toluamide; MNA, methylnicotinic acid; SLS, sodium lauryl sulfate.

the matrix of m covariate values for each of the n subjects, whereas Y is the dependent variable of interest. $h^* = 3(m + 1)/n$, where, in this case, m is the number of model variables and n is the number of objects used to calculate the model. The AD is the area of the plot where $h < h^*$ (Gramatica, 2007; Papa *et al.*, 2005).

RESULTS

The best MFs of those evaluated were HBAcceptor (the number of hydrogen bond acceptors) and 1/MP (the inverse of the MP) for PSFT and IPPSF biological systems, respectively. Tables 6, 7, and 8 present the final LFER model fits for PSFT and IPPSF experiments for both MFs in both models. Figures 1–6 illustrate the goodness of fit (including training data and validation data points) of the Abraham’s LFER model with no MF and best MF and the Williams’ leverage plot showing the chemical AD for the final MF-containing model for PSFT and IPPSF fits, respectively.

As can be seen from examining goodness of fit statistics as well as observed versus predicted plots, use of an MF in both systems significantly improved the ability of an LFER QSPR model to describe compound permeability compared with models that ignored the application mixture. This is best evidenced in the general improvement of r^2 and q^2 statistics when comparing models. In models that do not take into account mixture composition, the only predictor of the normalized absorptive flux k_p^* are the physicochemical properties of the penetrant molecules that determine the slope of the mean regression relation. In addition, this results in the plots of Figures 1 and 4 having columns of data located at the penetrant’s descriptor values, where the vertical height of each penetrant’s column reflects the vehicle effect. In many cases, this vehicle effect is greater than the vertical component of the slope resulting from mean permeability. As can be seen in Tables 6, 7, and 8, the MF is not LFER model dependent as fits were also improved when the data were analyzed using the model of Potts and Guy (1992).

A closer examination of the data presented in Tables 6, 7, and 8 for PSFT versus IPPSF model systems illustrates that different optimal MFs are needed for each model, with HBAcceptor being best for the PSFT and 1/MP best for the IPPSF data. In addition, if one examines the SE of the molecular descriptor coefficients, as well as the resultant p values, across models, it becomes evident that $\Sigma \beta_2^H$ (hydrogen bond acceptor basicity) in the PSFT and π_2^H (dipolarity/polarizability) in the IPPSF models have errors that exceed the mean, with p values greater than $\alpha = 0.05$, suggesting that these descriptors are not needed in the base LFER equation. We have reported the models with and without these terms. This is supported when these parameters are removed from the equations and the analysis repeated using the reduced model of Abraham and Martins.

The ability of the models to predict the validation data sets was determined by the external validation parameter (q_{EXT}^2).

TABLE 6
LFER Values for Pig Skin Diffusion Cells (PSFT) Log k_p ($n = 384$)—Abraham and Martins (2004) Model

| r^2 | Adj. r^2 | q_{LOO}^2 | $q_{\text{L25\%}}^2$ | q_{EXT}^2 | s | F | i | m | MF | $a \times \Sigma \alpha_2^{\text{H}}$ | $b \times \Sigma \beta_2^{\text{H}}$ | $s \times \pi_2^{\text{H}}$ | $e \times R_2$ | $v \times V_x$ |
|-------|------------|--------------------|----------------------|--------------------|------|-----|-------------|-----------------------------------|----|---------------------------------------|--------------------------------------|-----------------------------|----------------|----------------|
| 0.53 | 0.52 | 0.51 | 0.51 | 0.41 | 0.36 | 83 | 2.55(0.19) | No MF | | -1.45(0.21) | 0.01(0.14) | 0.27(0.12) | -0.55(0.13) | -1.39(0.09) |
| | | | | | | | $p < 0.001$ | No MF | | $p < 0.001$ | $p = 0.933$ | $p = 0.020$ | $p < 0.001$ | $p < 0.001$ |
| 0.71 | 0.70 | 0.69 | 0.69 | 0.44 | 0.23 | 151 | 3.14(0.15) | $77.66(5.08) \times 1/\text{MP}$ | | -1.47(0.17) | -0.01(0.11) | 0.27(0.09) | -0.56(0.10) | -1.39(0.07) |
| | | | | | | | $p < 0.001$ | $p < 0.001$ | | $p < 0.001$ | $p = 0.963$ | $p = 0.004$ | $p < 0.001$ | $p < 0.001$ |
| 0.73 | 0.73 | 0.73 | 0.72 | 0.61 | 0.21 | 173 | 4.25(0.17) | $-1.21(0.07) \times \text{HBacc}$ | | -1.40(0.16) | 0.03(0.10) | 0.27(0.09) | -0.55(0.10) | -1.38(0.07) |
| | | | | | | | $p < 0.001$ | $p < 0.001$ | | $p < 0.001$ | $p = 0.748$ | $p = 0.002$ | $p < 0.001$ | $p < 0.001$ |
| 0.73 | 0.73 | 0.72 | 0.72 | 0.61 | 0.20 | 208 | 4.27(0.16) | $-1.21(0.07) \times \text{HBacc}$ | | -1.44(0.11) | No $\Sigma \beta_2^{\text{H}}$ | 0.28(0.09) | -0.55(0.10) | -1.38(0.07) |
| | | | | | | | $p < 0.001$ | $p < 0.001$ | | $p < 0.001$ | No $\Sigma \beta_2^{\text{H}}$ | $p = 0.001$ | $p < 0.001$ | $p < 0.001$ |

Note. SE in parentheses. HBacc, number of hydrogen bond acceptors (calculated by www.molinspiration.com); 1/MP, inverse of the melting point (literature values from Syracuse University PhysProp Database <http://esc.syrres.com/interkow/physdemo.htm>).

Tables 6, 7, and 8 list the q_{EXT}^2 for each model. In the PSFT section of Tables 6, 7, and 8, it can be seen that the model with the best MF resulted in a $q_{\text{EXT}}^2 = 0.61$, whereas the IPPSF model with the best MF resulted in a $q_{\text{EXT}}^2 = 0.81$. The PSFT validation set used was not as well predicted by the equation determined from the training set as the validation data set predicted by the IPPSF model. This is largely a function of the validation sets used, which were data previously conducted by our laboratory which included different marker and mixture components. The training sets were full factorial combinations more balanced for model definition. The q_{LOO}^2 and $q_{\text{L25\%}}^2$ statistics support the use of these models in the training sets consisting of similar penetrants and mixture components. In contrast, the validation sets are relatively imbalanced yet provide a broader chemical diversity in terms of both penetrants and mixture components.

Finally, the Williams' plots for both final models (Fig. 3 for PSFT and Fig. 6 for IPPSF data) indicate that the training and validation compounds fall within an appropriate chemical AD for the model defined by the descriptors of the model and modeled response. Data points for which a compound or mixture are not appropriate based on the defined model would fall to the right of the critical hat value (h^*) and be excluded

from the analysis. This provides an easy test of whether an unknown compound has a reasonable chance to be included in the AD of an existing analysis.

CONCLUSIONS

These studies clearly demonstrate that components of a topical chemical mixture may modulate the dermal absorption of penetrants dosed in a mixture. In addition, the approach of using a composite MF, which takes into account the physical chemical properties of the mixture, allows for a mixture's potential effect on absorption to be quantitated in the framework of an accepted QSPR dermal absorption model. We use an LFER approach because numerous basic and theoretical studies have shown that multiple mechanisms of chemical penetration through skin may be operative preventing use of a single parameter to adequately predict absorption of a wide variety of substances. We have chosen the model of Abraham and Martins because of its wide use in this field. Recent work on diffusion cell studies have shown that one can formulate a reduced QSPR model based on simultaneous analysis of both penetrant and mixture data (Ghafourian *et al.*,

TABLE 7
LFER Values for Isolated Perfused Porcine Skin (IPPSF) LogAUC ($n = 119$)—Abraham and Martins (2004) Model

| r^2 | Adj. r^2 | q_{LOO}^2 | $q_{\text{L25\%}}^2$ | q_{EXT}^2 | s | F | i | m | MF | $a \times \Sigma \alpha_2^{\text{H}}$ | $b \times \Sigma \beta_2^{\text{H}}$ | $s \times \pi_2^{\text{H}}$ | $e \times R_2$ | $v \times V_x$ |
|-------|------------|--------------------|----------------------|--------------------|------|-----|-------------|-----------------------------------|----|---------------------------------------|--------------------------------------|-----------------------------|----------------|----------------|
| 0.60 | 0.58 | 0.56 | 0.56 | 0.72 | 0.15 | 34 | 1.61(0.34) | No MF | | -2.00(0.34) | -0.39(0.14) | 0.04(0.14) | 0.38(0.21) | -1.54(0.15) |
| | | | | | | | $p < 0.001$ | No MF | | $p < 0.001$ | $p = 0.005$ | $p = 0.774$ | $p = 0.067$ | $p < 0.001$ |
| 0.62 | 0.60 | 0.57 | 0.57 | 0.70 | 0.14 | 30 | 1.91(0.36) | $-0.27(0.12) \times \text{HBacc}$ | | -2.02(0.33) | -0.41(0.14) | 0.07(0.14) | 0.38(0.20) | -1.55(0.15) |
| | | | | | | | $p < 0.001$ | $p = 0.028$ | | $p < 0.001$ | $p = 0.003$ | $p = 0.610$ | $p = 0.062$ | $p < 0.001$ |
| 0.69 | 0.68 | 0.66 | 0.66 | 0.81 | 0.12 | 42 | 1.79(0.30) | $35.93(6.20) \times 1/\text{MP}$ | | -2.02(0.30) | -0.40(0.12) | 0.09(0.13) | 0.38(0.18) | -1.57(0.14) |
| | | | | | | | $p < 0.001$ | $p < 0.001$ | | $p < 0.001$ | $p = 0.001$ | $p = 0.475$ | $p = 0.039$ | $p < 0.001$ |
| 0.69 | 0.68 | 0.66 | 0.66 | 0.81 | 0.12 | 51 | 1.81(0.30) | $35.63(6.17) \times 1/\text{MP}$ | | -2.01(0.30) | -0.35(0.10) | No π_2^{H} | 0.47(0.13) | -1.61(0.13) |
| | | | | | | | $p < 0.001$ | $p < 0.001$ | | $p < 0.001$ | $p < 0.001$ | No π_2^{H} | $p = 0.001$ | $p < 0.001$ |

Note. SE in parentheses. HBacc, number of hydrogen bond acceptors (calculated by www.molinspiration.com); 1/MP, inverse of the melting point (literature values from Syracuse University PhysProp Database <http://esc.syrres.com/interkow/physdemo.htm>).

TABLE 8
LFER Values for Pig Skin Diffusion Cells (PSFT) $\text{Log}k_p$ ($n = 384$)—Potts and Guy (1992) Model

| r^2 | Adj. r^2 | q_{LOO}^2 | $q_{\text{L25\%}}^2$ | q_{EXT}^2 | s | F | i | m | MF | $a \times \log K_{\text{ow}}$ | $b \times \text{MW}$ |
|-------|------------|--------------------|----------------------|--------------------|------|-----|-------------|-----------------------------------|----|-------------------------------|----------------------|
| 0.33 | 0.33 | 0.32 | 0.32 | NA | 0.51 | 94 | 1.13(0.13) | No MF | | -0.10(0.02) | -0.0058(0.0006) |
| | | | | | | | $p < 0.001$ | No MF | | $p < 0.001$ | $p < 0.001$ |
| 0.55 | 0.54 | 0.54 | 0.54 | NA | 0.35 | 152 | 2.89(0.17) | $-1.23(0.09) \times \text{HBAcc}$ | | -0.10(0.02) | -0.0058(0.0005) |
| | | | | | | | $p < 0.001$ | $p < 0.001$ | | $p < 0.001$ | $p < 0.001$ |

Note. SE in parentheses. HBAcc, number of hydrogen bond acceptors (calculated by www.molinspiration.com); 1/MP, inverse of the melting point (literature values from Syracuse University PhysProp Database <http://esc.syrres.com/interkow/physdemo.htm>). NA, not applicable.

2010); however, our goal was to determine how a mixture impacts on a QSPR model determined from single penetrants that is widely adopted in risk assessments.

These studies involve toxicologically relevant lipophilic compounds studied across various vehicles using an albumin-containing perfusate that contrasts with the more hydrophilic drugs dosed in aqueous vehicles using aqueous receptor fluids studied in other QSPR analyses largely targeted to drug development endpoints. Our focus is to develop an approach to handle vehicle interactions, which would be applicable to other data sets and be relevant to occupational and/or environmental exposure scenarios. Our study chemicals are relatively more lipophilic than those modeled in many QSPR studies, which were designed to predict absorption of relatively hydrophilic drug molecules (Ghafourian *et al.*, 2010). Investigators have long known that there exists a parabolic relationship between the flux of chemicals across skin and $\log K_{\text{ow}}$, peaking at a $\log K_{\text{ow}}$ of approximately 2–3, a value approximating the lipophilicity of the stratum corneum barrier lipids (Cross *et al.*, 2003b; Roberts and Walters, 1998; Scheuplein and Blank, 1971). In fact, it has been shown that this relationship shifted to a lower $\log K_{\text{ow}}$ when lauric acid was added to an aqueous

ethanol vehicle (Lee *et al.*, 1994), supporting the MF concept that vehicles modulate the $k_p - K_{\text{ow}}$ relationship. Permeability of more lipophilic penetrants in any vehicle becomes increasingly reduced because of resistance from dermal elements. Another difference with our work and those targeted toward drug delivery is that our studies use albumin-containing perfusate. This facilitates absorption of lipophilic compounds (Bronaugh and Stewart, 1984; Cross *et al.*, 2003a) and generates data that can be directly compared across both PSFT and IPPSF model systems because the vascularized IPPSF requires albumin in the perfusate to maintain sufficient oncotic pressure to maintain capillary perfusion. Finally, use of albumin-containing perfusate is also more closely related to the *in vivo* scenario.

We estimate transdermal absorption in the PSFT system using an operational or apparent k_p^* determined from the initial applied surface concentration in a specific mixture and the observed pseudo-steady state flux. We do not estimate a true steady state flux from an infinite dose exposure. Likewise, we do not conduct the studies occluded, which although would prevent evaporative loss, also occludes the stratum corneum barrier altering its inherent permeability. Finally, as discussed

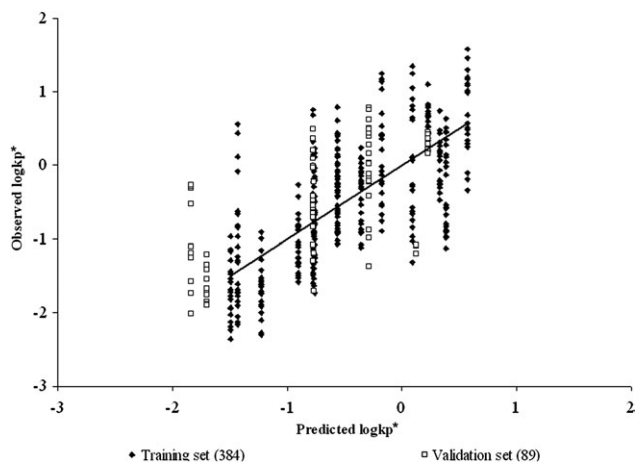


FIG. 1. Model of Abraham and Martins of the PSFT training and validation set data with no MF. $r^2 = 0.53$, adj. $r^2 = 0.52$, $q_{\text{LOO}}^2 = 0.51$, $q_{\text{L25\%}}^2 = 0.51$, and $q_{\text{EXT}}^2 = 0.41$.

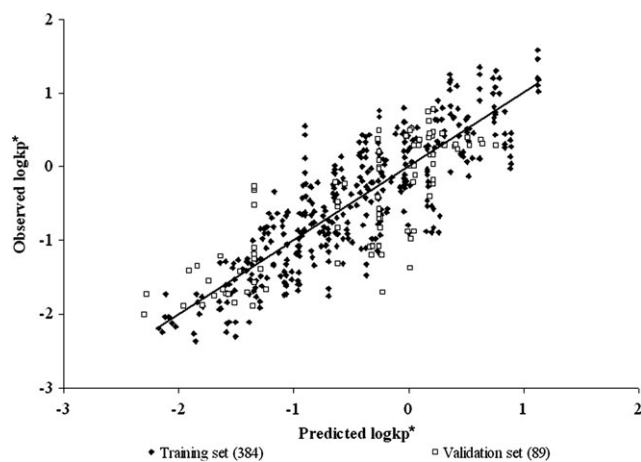


FIG. 2. Model of Abraham and Martins of the PSFT training and validation set data with MF = HBAcc (the number of hydrogen bond acceptors). $r^2 = 0.73$, adj. $r^2 = 0.73$, $q_{\text{LOO}}^2 = 0.73$, $q_{\text{L25\%}}^2 = 0.72$, and $q_{\text{EXT}}^2 = 0.61$.

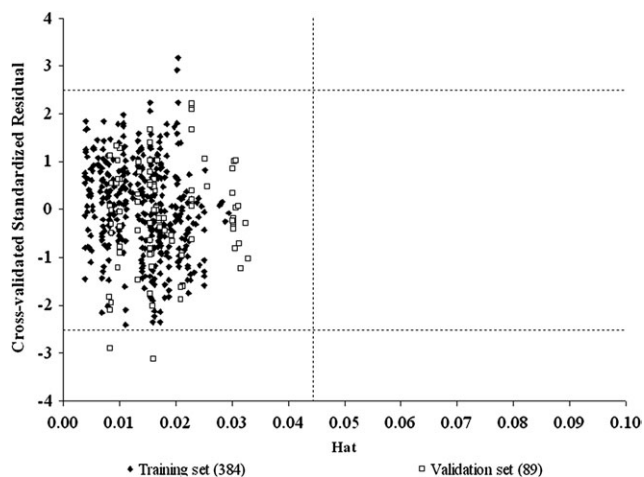


FIG. 3. Williams' leverage validation plot of the model of Abraham and Martins of the PSFT training and validation set data with MF = HBAcc (the number of hydrogen bond acceptors). $h^* = [3(6 + 1)]/473 = 0.044$.

above, albumin is present in the media that alters the dermal penetration phenomenon away from those conditions that would be optimal to define a true Fickian permeability coefficient. The conditions employed in our study closely mimic natural occupational or environmental exposures. Unlike the design inherent to infinite dose studies, skin is not prehydrated in our experiments. Differences in the vehicle effects on percutaneous absorption of lactic acid were seen under finite versus infinite dosing designs (Sah *et al.*, 1998). We hypothesize that the nature of our MF identifies rate-limiting processes involved in modulating penetrant absorption from a complex vehicle (e.g., altered solubility, binding, etc.) that may differ from exposures dosed under more artificial conditions.

One approach, which has been used to predict absorption from complex vehicle mixtures, is to experimentally estimate

maximum flux determined from a saturated solution of a penetrant in a study mixture, a scenario that reflects maximum thermodynamic activity of the penetrants (Cross *et al.*, 2001). This exposure scenario would be expected to be predictive of subsequent dermal absorption from a saturated solution; however, it may not be applicable to nonsaturated solutions and requires experimental studies, making the approach not amenable to estimating absorption from different mixtures, a major goal of our approach.

The primary finding of the present study is the difference in QSPR model structure between PSFT and IPPSF experiments, which implies different modulating factors in a system whose absorptive flux is primarily restricted by stratum corneum resistance (PSFT) versus one which also has dermal and vascular elements present (IPPSF). This is evidenced both by the requirement of different base QSPR descriptors needed for the systems (no $\Sigma\beta_2^H$ in PSFT and no π_2^H in IPPSF) as well as the different MFs for both systems (Tables 6, 7, and 8). This comparison is relatively robust because all exposures use porcine skin from the same strain of pigs, use identical dosing conditions (concentration, finite dose, and no occlusion) to mimic *in vivo* exposures, and use the same perfusate and analytical technique.

This finding has many implications beyond its relevance to predicting absorption from a mixture in two different experimental model systems because the implication is clearly that physicochemical factors that are rate limiting in the simpler *in vitro* system may not be directly transferable to the more complex perfused skin system and, by extension, to the *in vivo* exposure scenario. Obvious differences would include interactions with dermal elements in the vascularized model, which are not operative in the diffusion cell system. The pharmacokinetics of penetration through a dermatomed skin model versus an intact epidermal-dermal skin barrier may also be significantly different and affect rate-limiting processes

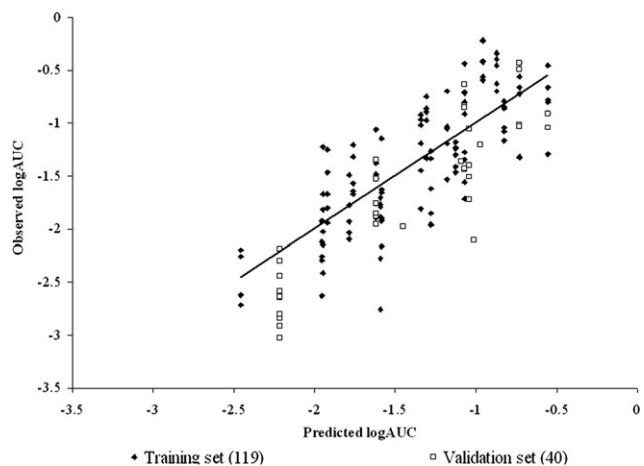


FIG. 4. Model of Abraham and Martins of the IPPSF training and validation set data with no MF. $r^2 = 0.60$, adj. $r^2 = 0.58$, $q_{LOO}^2 = 0.56$, $q_{L25\%}^2 = 0.56$, and $q_{EXT}^2 = 0.72$.

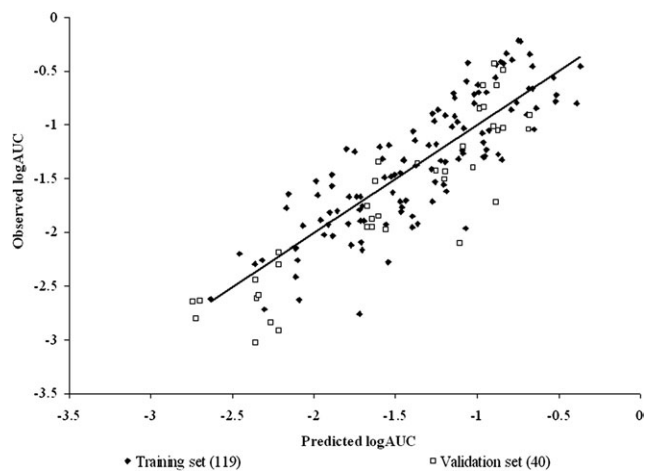


FIG. 5. Model of Abraham and Martins of the IPPSF training and validation set data with MF = 1/MP (the inverse of the MP). $r^2 = 0.69$, adj. $r^2 = 0.68$, $q_{LOO}^2 = 0.66$, $q_{L25\%}^2 = 0.66$, and $q_{EXT}^2 = 0.81$.

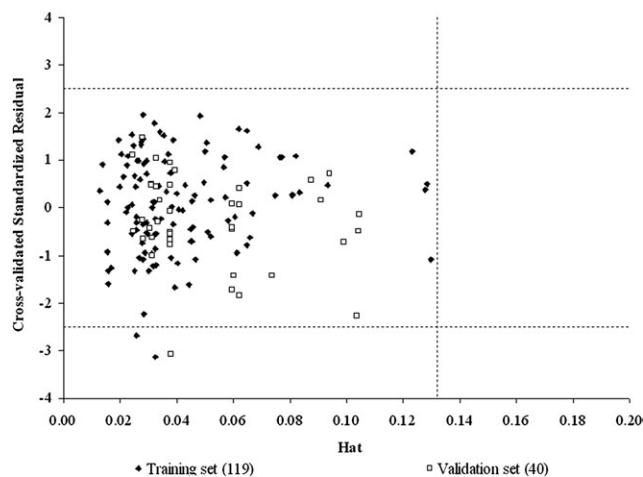


FIG. 6. Williams' leverage validation plot of the model of Abraham and Martins of the IPPSF training and validation set data with $MF = 1/MP$ (the inverse of the MP). $h^* = [3(6 + 1)]/159 = 0.1321$.

detectable in this pseudo-steady state experiment. All vehicle effects may not exhibit this biological system dependency, as we recently showed when low-level single-dose surfactant effects on dermal absorption in the IPPSF could be predicted from an inert membrane fiber model (Riviere *et al.*, 2010), suggesting only solution effects were operative.

The MF approach confounds solvatochromatic effects of penetrant-vehicle interactions in solution (altered solubility, etc.) with vehicle interactions with the skin barrier. Workers have previously shown that vehicle pretreatment modulates subsequent absorption (Rosado *et al.*, 2003). Although this reduces the ability of the model to assign specific mechanisms for the mixture effects seen, it also is more relevant in determining the nature of the effects expected when *in vivo* exposures to complex mixtures occur. The difference in both underlying model structure (four- vs. five-term model) and different MFs selected suggests that the rate-limiting process for a mixture's effect on absorption differs between the two biological systems studied, implying vehicle effects on skin and not simply solubility effects in solution, which is controlled across our biological systems. In our previous analysis of these data using a smaller set of penetrants, a similar phenomenon was detected where the best factors for PSFT were refractive index and TPSA of mixture components, whereas for IPPSF, it was log water solubility and ovality. The present study, consisting of a much larger number of chemicals conducted under identical controlled conditions, allows a specific test of this hypothesis to be conducted.

There are several implications resulting from this study. The most obvious conclusion is that knowledge of permeability from a simple vehicle is not sufficient to predict absorption from a more complex multicomponent vehicle. This is best seen comparing Figures 1, 2, 4, and 5. In many cases, the vertical height of the penetrant-specific columns in Figures 1 and 4 are greater than the vertical rise determined

from the slope of the predicted absorptive flux for that penetrant. The vehicle effect dominates over inherent permeability. This is the scenario that this research is attempting to consider. The second implication is that the nature of the optimal QSPR model for *in vitro* diffusion cells versus an *ex vivo* isolated perfused skin model is different, suggesting that different rate-limiting processes are operative in both systems. This has a direct effect on using *in vitro* data to estimate *in vivo* exposures. For both implications, absorption data from a specific formulation or mixture exposure would be preferred and when available should be used. In the case when no data except knowledge of an apparent k_p^* or absorptive flux from a single vehicle exposure in an *in vitro* system are available, an approach such as discussed in this paper needs to be developed.

FUNDING

National Institute of Occupational Safety and Health Grant (R01 07555).

REFERENCES

- Abraham, M. H., and Martins, F. (2004). Human skin permeation and partition: general linear free-energy relationship analyses. *J. Pharm. Sci.* **93**, 1508–1523.
- Augustijns, P. and Brewster, M. E., Eds. (2007). *Solvent Systems and Their Selection in Pharmaceuticals and Biopharmaceutics*. Springer, New York, NY.
- Baynes, R. E., Xia, X. R., Imram, M., and Riviere, J. E. (2008). Quantification of chemical mixture interactions that modulate dermal absorption using a multiple membrane coated fiber array. *Chem. Res. Toxicol.* **21**, 591–599.
- Bliss, C. I. (1939). The toxicity of poisons applied jointly. *Ann. Appl. Biol.* **26**, 585–615.
- Bowman, K. F., Monteiro-Riviere, N. A., and Riviere, J. E. (1991). Development of surgical techniques for preparation of *in vitro* isolated perfused porcine skin flaps for percutaneous absorption studies. *Am. J. Vet. Res.* **52**, 75–82.
- Bronaugh, R. L., and Stewart, R. F. (1984). Methods for *in vitro* percutaneous absorption studies III. Hydrophobic compounds. *J. Pharm. Sci.* **73**, 1255–1258.
- Bronaugh, R. L., and Stewart, R. F. (1985). Methods for *in vitro* percutaneous absorption studies IV. The flow-through diffusion cell. *J. Pharm. Sci.* **74**, 64–67.
- Chang, S. K., and Riviere, J. E. (1991). Percutaneous absorption of parathion *in vitro* in porcine skin. Effects of dose, temperature, humidity and perfusate composition on absorptive flux. *Fundam. Appl. Toxicol.* **17**, 494–504.
- Cross, S. E., Anissimov, Y. G., Magnusson, B. M., and Roberts, M. S. (2003a). Bovine serum albumin containing receptor phase better predicts transdermal absorption parameters for lipophilic compounds. *J. Invest. Dermatol.* **120**, 589–591.
- Cross, S. E., Magnusson, B. M., Winckle, G., Anissimov, Y., and Roberts, M. S. (2003b). Determination of the effect of lipophilicity on the *in vitro* permeability and tissue reservoir characteristics of topically applied solutes in human skin layers. *J. Invest. Dermatol.* **120**, 759–764.

- Cross, S. E., Pugh, W. J., Hadgraft, J., and Roberts, M. S. (2001). Probing the effects of vehicles on topical delivery. *Pharm. Res.* **18**, 999–1005.
- Environmental Protection Agency (EPA) (2004). *Risk Assessment Guidance for Superfund. Volume I: Human Health Evaluation Manual (Part E, Supplemental Guidance for Dermal Risk Assessment)*. EPA/540/R/99/005, July 2004. pp. 3–1 to 3–10. U.S. Environmental Protection Agency, Washington, DC.
- Geinoz, S., Guy, R. H., Testa, B., and Carrupt, P. A. (2004). Quantitative structure permeation relationships (QSPeR) to predict skin permeation: a critical evaluation. *Pharm. Res.* **21**, 83–92.
- Ghafourian, T., Samaros, E., Brooks, J. D., and Riviere, J. E. (2010). Modeling the effects of mixture components on skin permeation. *Int. J. Pharm.* **398**, 28–32.
- Gramatica, P. (2007). Principles of QSAR models validation: internal and external. *QSAR Comb. Sci.* **26**, 694–701.
- Gregoire, S., Ribaud, C., Benech, F., Meunier, J. R., Garrigues-Mazert, A., and Guy, R. H. (2009). Prediction of chemical absorption into and through the skin from cosmetic and dermatological formulations. *Br. J. Dermatol.* **160**, 80–91.
- Hostynek, J. J., and Magee, P. S. (1997). Modeling in vivo human skin absorption. *QSAR* **16**, 473–479.
- Idson, B. (1983). Vehicle effects in percutaneous absorption. *Drug Metab. Rev.* **14**, 207–222.
- Lee, C. K., Uchida, T., Kitagawa, K., Yagi, A., Kim, N. S., and Goto, S. (1994). Relationship between lipophilicity and skin permeability of various drugs from an ethanol/water/lauric acid system. *Biol. Pharm. Bull.* **17**, 1421–1424.
- Monteiro-Riviere, N. A., Bowman, K. F., Scheidt, V. J., and Riviere, J. E. (1987). The isolated perfused porcine skin flap (IPPSF): II. Ultrastructural and histological characterization of epidermal viability. *In Vitro Toxicol.* **1**, 241–252.
- Neuman, D. (2008). Modeling transdermal absorption. In *Drug Absorption Studies* (Ehrhardt, C. and Kim, K., Eds.), pp. 459–485. Springer US, New York, NY.
- Papa, E., Villa, F., and Gramatica, P. (2005). Statistically validated QSARs, based on theoretical descriptors, for modeling aquatic toxicity of organic chemicals in *Pimephales promelas* (fathead minnow). *J. Chem. Inf. Model.* **45**, 1256–1266.
- Potts, R. O., and Guy, R. H. (1992). Predicting skin permeability. *Pharm. Res.* **9**, 663–669.
- Qiao, G. L., Brooks, J. D., Baynes, R. E., Monteiro-Riviere, N. A., Williams, P. L., and Riviere, J. E. (1996). The use of mechanistically defined chemical mixtures (MDCM) to assess component effects on the percutaneous absorption and cutaneous disposition of topically-exposed chemicals. I. Studies with parathion mixtures in isolated perfused porcine skin. *Toxicol. Appl. Pharmacol.* **141**, 473–486.
- Riviere, J. E. (2006). Perfused skin models. In (Riviere, J. E., Ed.), *Dermal Absorption Models in Toxicology and Pharmacology*. New York, NY: Taylor and Francis/CRC Press. pp. 27–45.
- Riviere, J. E., Bowman, K. F., Monteiro-Riviere, N. A., Dix, L. P., and Carver, M. P. (1986). The isolated perfused porcine skin flap (IPPSF). I. A novel in vitro model for percutaneous absorption and cutaneous toxicology studies. *Fundam. Appl. Toxicol.* **7**, 444–453.
- Riviere, J. E., and Brooks, J. D. (2005). Predicting skin permeability from complex chemical mixtures. *Toxicol. Appl. Pharmacol.* **208**, 99–110.
- Riviere, J. E., and Brooks, J. D. (2007). Prediction of dermal absorption from complex chemical mixtures: incorporation of vehicle effects and interactions into a QSPR framework. *SAR QSAR Environ. Res.* **18**, 31–44.
- Riviere, J. E., Brooks, J. D., Yeatts, J. L., and Koivisto, E. (2010). Surfactant effects on skin absorption of model organic chemicals: implications for dermal risk assessment studies. *J. Toxicol. Environ. Health Part A* **73**, 725–737.
- Riviere, J. E., and Monteiro-Riviere, N. A. (1991). The isolated perfused porcine skin flap as an in vitro model for percutaneous absorption and cutaneous toxicology. *Critic. Rev. Toxicol.* **21**, 329–344.
- Riviere, J. E., Williams, P. L., Hillman, R., and Mishky, L. (1992). Quantitative prediction of transdermal iontophoretic delivery of arbutamine in humans using the in vitro isolated perfused porcine skin flap (IPPSF). *J. Pharm. Sci.* **81**, 504–507.
- Roberts, M. S., and Walters, K. A. (1998). The relationship between structure and barrier function in skin. In *Dermal Absorption and Toxicity Assessment* (Roberts, M. S. and Walters, K. A., Eds.) pp. 1–42. Marcel Dekker Inc., New York.
- Rosado, C., Cross, S. E., Pugh, W. J., Roberts, M. S., and Hadgraft, J. (2003). Effect of vehicle pretreatment on the flux, retention, and diffusion of topically applied penetrants in vitro. *Pharm. Res.* **20**, 1502–1507.
- Sah, A., Mukherjee, S., and Wickett, R. R. (1998). An in vitro study of the effects of formulation variables and product structure on percutaneous absorption of lactic acid. *J. Cosmet. Sci.* **49**, 257–273.
- Scheuplein, R. J., and Blank, I. H. (1971). Permeability of the skin. *Physiol. Rev.* **51**, 702–747.
- Sloan, K. B., Koch, S. A. M., Siver, K. G., and Flowers, F. P. (1986). Use of solubility parameters of drug and vehicle to predict flux through skin. *J. Invest. Dermatol.* **87**, 244–252.
- Wester, R. C., Melendres, J., Sedik, L., Maibach, H. I., and Riviere, J. E. (1998). Percutaneous absorption of salicylic acid, theophylline, 2,4-dimethylamine, diethyl hexylphthalic acid and p-aminobenzoic acid in the isolated perfused porcine skin flap compared to man. *Toxicol. Appl. Pharmacol.* **151**, 159–165.